



Rheological behavior and modeling of an ultrafiltration process for Aloe vera

L. Medina-Torres¹  | I. H. González Guillen² | D. M. Núñez-Ramírez³ |
P. García-Guzmán⁴ | F. Calderas²  | R. F. González Laredo⁵ |
M. A. Gonzalez Lozano³ | L. A. Ramirez Torres⁶ | O. Manero⁶

¹Facultad de Química, Circuito Exterior, Universidad Nacional Autónoma de México, CDMX, Mexico

²Unidad de Bioingeniería L7 PP UMIÉZ, Facultad de Estudios Superiores-Zaragoza, Universidad Nacional Autónoma de México, CDMX, Mexico

³Facultad de Ciencias Químicas, Avenida Veterinaria S/N, Circuito Universitario, Universidad Juárez del Estado de Durango (UJED), Durango, Mexico

⁴Departamento de Sistemas Biológicos, Universidad Autónoma Metropolitana, Unidad Xochimilco, CDMX, Mexico

⁵Departamento de Ing. Química y Bioquímica, Instituto Tecnológico de Durango, Durango, Mexico

⁶Instituto de Investigaciones en Materiales, Universidad Nacional Autónoma de México, CDMX, Mexico

Correspondence

F. Calderas, Universidad Nacional Autónoma de México, Facultad de Estudios Superiores-Zaragoza, Iztapalapa, CDMX, 09230, México. Email: faustocg@unam.mx

L. Medina-Torres, Universidad Nacional Autónoma de México, Facultad de Química, Circuito Exterior, S/N, C.U., Coyoacán, 04510 CDMX 04510, México. Email: luismt@unam.mx

Abstract

Aloe vera (*Aloe barbadensis* Miller) is employed as a food supplement containing mucopolysaccharides which contribute to a healthy diet. Aloe vera mucilage is usually obtained through an evaporation process. An alternative process to preserve polysaccharide properties is ultrafiltration (UF), which impedes degradation of the compound by temperature. This work analyses the effect of the UF process on the mechanical and rheological properties of Aloe vera considering the following variables: temperature (T), input feeding rate (V), and transmembrane pressure (ΔPTM). The permeate flux varies according to the operating conditions exhibiting non-Newtonian effects. The determination of the mass transfer coefficient is based on the analogy of transport phenomena (heat transfer to mass transfer) in non-Newtonian fluids to obtain the permeate flux. The results show that when the mucilage is fed as a diluted shear-thinning fluid, the UF efficiency is positively affected. To describe the rheological behavior of the concentrated mucilage, the power law and the Bautista-Manero-Puig (BMP) models are used and compared. Results suggest that the BMP model represents better the experimental data of permeate flux as a function of filtrate concentration with respect to the experimentally measured permeate flux.

Practical Applications

Currently, the use of Aloe vera mucilage as encapsulating agents, thickeners, emulsifiers, and wall materials is highly appreciated by the food and pharmaceutical industry. This research shows that the concentrate obtained from Aloe vera mucilage by ultrafiltration (UF) preserves its rheological properties, unlike other thermal processes. Results represent an interesting and promising alternative to estimate the

Abbreviations: e , Membrane thickness (m); ΔP , Transmembrane differential pressure (Pa); $\dot{\gamma}$, Shear rate (s^{-1}); φ_0 , Fluidity at zero shear rate ($Pa^{-1}s^{-1}$); φ_∞ , Fluidity at very high shear rates ($Pa^{-1}s^{-1}$); B , Exponent of the axial velocity term; C , Solute concentration near the membrane (% °Brix); C_b , Mucilage concentration (%); d , diameter of tubular membrane (m); D , Diffusive coefficient ($m^2 s^{-1}$); J , Permeate flow ($m^3 m^{-2} s^{-1}$); k , Convective mass transfer coefficient ($m h^{-1}$); K , kinetic constant of structure breakage; L , Membrane length (m); m , Consistency index ($Pa s^n$); n , Shear thinning index (–); n_b , m_b , m_w , Flow index (–) and consistency ($Pa s^n$) in the center and at the walls; R_{cp} , The concentration polarization resistance; Re , Reynolds number (–); R_g , The gel layer resistance.; R_m , Hydraulic resistance of the virgin membrane; T , Temperature ($^{\circ}C$); u , Velocity (m/s); UF, Ultrafiltration; v , Feed rate (m^3/s); V , Feeding rate (m^3/s); W , Weight (kg); ΔPTM , Transmembrane pressure (Pa); λ , structural relaxation time; α , Specific resistance of the membrane ($Pa s m^{-1}$); β , Kinetic-structural parameter ($Pa^{-1} s$); $\eta(\dot{\gamma})$, Apparent viscosity ($Pa s$); φ , Fluidity ($Pa^{-1} s^{-1}$).

This is an open access article under the terms of the [Creative Commons Attribution-NonCommercial-NoDerivs](https://creativecommons.org/licenses/by-nc-nd/4.0/) License, which permits use and distribution in any medium, provided the original work is properly cited, the use is non-commercial and no modifications or adaptations are made.

© 2023 The Authors. *Journal of Food Process Engineering* published by Wiley Periodicals LLC.

properties of Aloe vera using more realistic rheological models with promising applications in the food and pharmaceutical industry. The Aloe vera mucilage increases the health benefits using the mucilage in different concentrations in different industrial processes.

KEYWORDS

Aloe vera mucilage, modeling, permeate flux, rheology, ultra-filtration

1 | INTRODUCTION

Aloe vera (*Aloe barbadensis* Miller) mucilage is a natural plant used as a nutritional supplement for its anti-inflammatory and analgesic properties in treating burns and alleviating pain caused by rheumatoid arthritis. Aloe vera mucilage is considered a potential source of hydrocolloids that can provide nutritional additives in the production of nutraceutical products (Cervantes et al., 2014; Rodríguez-Rodríguez et al., 2010). The usual commercial presentation of Aloe vera is as a diluted-form mucilage (Cervantes et al., 2014; Rodríguez-Rodríguez et al., 2010; Vega et al., 2005) containing 99% water and only 1.0% solids. It is composed of at least four different partial acetylated glucmannans, which differ in their glucose to mannose ratio and acetyl content. Aloe vera mucilage composition comprises D-glucose and D-mannose with 24% of uronic acid (Femenia et al., 1999; Femenia et al., 2003). The Aloe vera mucilage contains 55.2 mg of polysaccharides per 100 mL. The approximate total mass of polysaccharides is 13% (788 mg/L) (Cervantes et al., 2014; Cheryan, 1986; Femenia et al., 1999; Femenia et al., 2003; Pizzichini, 1995; Rodríguez-Rodríguez et al., 2010 and Vega et al., 2005).

The mucopolysaccharides are important elements of Aloe vera mucilage. Femenia et al. (1999) reported that the polysaccharides are contained in the parenchyma (i.e., the typical cellular tissue that is soft and succulent, found mainly in leaves) of the Aloe vera plant. The main and bioactive carbohydrate in Aloe vera is acemannan which is rich in mannose and glucose, that is, high molecular weight polysaccharides. These polysaccharides vary in size and do not form real aqueous solutions; in fact, they form colloidal emulsions that decompose via hydrolysis reactions in the cellular matrix of the Aloe vera plant. These bioactive polysaccharides have been reported to possess antibacterial, antiviral, antifungal, and antiparasitic properties that enhance the response of the human immune system to some diseases when consumed in appropriate quantities (Femenia et al., 1999, Femenia et al., 2003). Due to the high-water activity of the Aloe vera mucilage ($a_w > 0.90$), its shelf-life period lasts 3–4 days at room temperature. Increasing the life span is required for industrial processing and applications (Cervantes et al., 2014; Rodríguez-Rodríguez et al., 2010).

The use of membrane technology in the UF processes of such polysaccharides offers the sensorial attributes of the natural products with no thermal treatment that may decompose the product. The UF process reduces the use of chemical additives, avoiding strong varia-

tions in temperature and degradation of fluid components (Muller, 1982; Nakao et al., 1979). This process employs a semi-permeable membrane with a pressure gradient at both sides of the membrane to separate high molecular weight particles, allowing the diffusion of small molecules through the membrane pores (i.e., “permeate” or “filtrate”).

The flux is the rate at which the fluid passes through the membrane area and a concentrate product is obtained at the end of the process (Chou et al., 1991; Mears, 1976). UF processes are used to separate dissolved solutes ranging from 0.002 to 0.2 microns in size, corresponding to molecular weights of 50–300,000 Da (Charcosset & Choplin, 1996; Chou et al., 1991; Mears, 1976), which is lies range of the polysaccharides contained in Aloe vera mucilage.

2 | MASS TRANSFER IN THE MEMBRANE CONCENTRATION POLARIZATION LAYER

Ultrafiltration modeling involves mass-transfer coefficient correlations to characterize the mass transfer process through a membrane. In ultrafiltration processes, the permeate flow through the membrane is given by the following equation (Cui et al., 2010; Lim & Mohammad, 2012):

$$J = \frac{\Delta P}{\alpha e}, \quad (1)$$

where J is the permeate flux (m/s), α is a specific resistance of the membrane (Pa s/m^2), e is the membrane thickness (m), and ΔP is the membrane differential pressure (Pa). Since α is proportional to the viscosity in laminar flow, J can be rewritten as:

$$J = \frac{\Delta P}{\eta R_t}, \quad (2)$$

where η is the fluid viscosity (Pa s) and R_t is the total filtration resistance (m^{-1}).

Considering that the increase in solute concentration near the membrane reduces the effective transmembrane pressure by increasing the osmotic pressure (i.e., concentration polarization), equation (2) becomes:

$$J = \frac{\Delta P - \Delta \Pi}{\eta R_t}, \quad (3)$$

If membrane fouling is considered, the flux is represented as a series of resistances:

$$J = \frac{\Delta P - \Delta \Pi}{\eta(R_m + R_{cp} + R_g)}, \quad (4)$$

where R_m is the hydraulic resistance of the pristine membrane, R_{cp} is the concentration polarization resistance and R_g is the gel layer resistance.

Usually, in the UF process, a gel is generated on the membrane surface which concentration increases with time. This concentration effect is called polarization, representing a constant decrease in permeate flow with time. When this permeates flow significantly decreases, it renders the whole operation unprofitable (Lim & Mohammad, 2012; Cui & Muralidhara, 2010).

To obtain the concentration profile, the flux of solute (mass transfer) due to both convection and diffusion (making an analogy to heat flow) through the boundary layer is equal to the flux of solute in the permeate:

$$Jc + D_J \frac{dc}{dx} = Jc_2, \quad (5)$$

Equation (5) is integrated with boundary conditions $c = c_w$ at $x = 0$ and $c = c_b$ at $x = \delta$, the thickness of the boundary layer. The term D/δ is the mass transfer coefficient k_c :

$$\ln \frac{c_w - c_2}{c_b - c_2} = \frac{J\delta}{D} = \frac{J}{k_c} \quad (6)$$

For the case of complete rejection of the solute ($c_2 = 0$), Equation (6) becomes

$$J = k_c \ln \frac{c_w}{c_b}. \quad (7)$$

Due to concentration polarization, the permeate flux is a non-linear function of ΔP and a trial-and-error solution is needed to calculate J for a given ΔP . However, when complete rejection of the solute holds and there is no gel strength, Δp can be obtained for a given J directly using Equation (7) to obtain c and the osmotic pressure data to obtain $\Delta \Pi$, which adds to the term $(\Delta P - \Delta \Pi)$ in Equation (4) to give ΔP .

UF processes are commonly carried out under tangential flow conditions, yielding adequate product volumes for various flow conditions. In the conventional filtering process, the flow direction is normal to the surface and clogging occurs faster than in the tangential flow filtration (ultrafiltration) (Chou et al., 1991; Mears, 1976).

Previous studies have reported the effect of the rheological properties of non-Newtonian fluids in ultrafiltration processes (Aimar, 1987; Mondal et al., 2016; Pritchard, 1990), revealing that fluids with shear-thinning behavior (viscosity decreasing with shear rate) cause increasing mass transfer rates as compared with those of Newtonian fluids (constant viscosity). An important factor to consider is the change in permeate viscosity with concentration which, in the

case of shear thinning fluids, has been reported to shift the viscosity curve in the y direction when plotted versus the shear rate but maintaining the slope of the curve (Aimar, 1987; Pritchard, 1990; Mondal et al., 2016). Studies on the UF process in non-Newtonian fluids using a highly viscous fluid and a shear-thinning liquid permeate have reported that UF process feeds with low content of concentrated pseudoplastic solutions at high shear led to a more permeated flow mass, since highly concentrated pseudoplastic solutions tend to decrease feeding speeds when the flux is varied.

The main objective of this work is the analysis of the influence of the mucilage rheological properties on the UF process, employing more adequate rheological models for the complex flow occurring in the ultrafiltration model to better understanding and higher accuracy in the prediction of the permeate flux. Theoretical predictions of the permeate flux consistent with the experimental values of an inelastic shear-thinning non-Newtonian fluid (i.e., Aloe vera mucilage) facilitates the design and optimization of UF equipment of concentrated Aloe vera mucilage with applications in the chemical and food industries.

The Bautista-Manero-Puig (BMP) model (Bautista et al., 1999) is employed to describe the UF process (Charcosset & Choplin, 1996). This model adequately describes the nonlinear behavior of complex fluids considering structure parameters. It consists of the upper convective Maxwell Equation (8a) and a kinetic equation that describes the structural change induced by the flow:

$$\underline{\underline{\tau}} + \delta(r, t) \frac{\nabla}{\underline{\underline{\tau}}} = \frac{2D}{\varphi(r, t)}, \quad (8a)$$

$$\frac{d\varphi}{dt} = \frac{1}{\lambda}(\varphi_0 - \varphi) + K(\varphi_\infty - \varphi) \underline{\underline{\tau}} : \underline{\underline{D}}, \quad (8b)$$

where φ is the fluidity ($\equiv \eta^{-1}$, inverse viscosity), φ_0 and φ_∞ are the fluidities at small and high shear rates, respectively; λ is a structural relaxation time and K can be interpreted as a kinetic constant for the breakage of the structure [21]. $\frac{\nabla}{\underline{\underline{\tau}}}$ is the upper convective derivative of the stress tensor, $\delta = [(G_0 \varphi)^{-1}]$ is the structure-dependent relaxation time and G_0 is the instantaneous relaxation modulus.

Permeate flux predictions of the UF process using the power law and BMP models are compared. These models predict a shear-thinning viscosity with a slope which remains constant when the viscosity increases (concentration changes). In addition, the BMP model describes shear thinning phenomena including a viscosity plateau at low and high shear rates (Constant viscosity behavior), whereas the power law model only describes the shear thinning region. Pritchard (1990) proposed an expression for a mass transfer coefficient, which incorporates the effect of pseudoplasticity based on the integration of the model proposed by Field:

$$k = \left(\frac{3D^2}{4L} \right)^{\frac{1}{2}} \left(\frac{3n_b + 1}{4n_b} \right)^B \left(\frac{r_b}{m_b m_w^{n_w} r_w^{0.13}} \right)^B, \quad (9a)$$

where n_b , n_w , m_b , and m_w represent the flow index (n) and consistency (m) at the center (b) and walls (w) of the pipe, and B is the exponent of the axial velocity term:

$$B = 2n_b/3(n_b + n_w). \quad (9b)$$

Such formulation assumes laminar flow conditions, with no slip at the walls. The shear rate depends only on the shear stress, using cross-flow membrane filtration models. This equation describes the increase in the laminar flow mass transfer coefficient with xanthan concentration (Charcosset & Choplin, 1996). However, this correlation is not suitable in the case where K_w is quite different to K_b , and it is valid only when the pseudoplasticity indices n_b and n_w are equal.

Finally, this study focuses on the evaluation of the effect of the mucilage concentration on the rheological properties of the filtrate obtained from the UF process. The novelty of this work with respect to those reported by Charcosset and Choplin (1996), on the UF process with Xhantan and polyacrylamide, is to demonstrate the feasibility to concentrate the Aloe vera mucilage using UF while preserving the structure and properties of the original compound, as revealed in the rheological characteristics of the filtrate.

3 | EXPERIMENTAL

3.1 | Raw materials

Aloe vera leaves were collected from a semiarid region in Durango, Mexico. The Aloe vera sword-like, 24–30 months old leaves have dimensions of 2–3 cm thick, 10–12 cm wide, and 25–30 cm large, prior to flourishing. The leaves have a smooth, soft, and flexible surface, with sharp, slightly yellow spines at the edges oriented toward the apex. Bright green leaves (with no visible spots) were taken from the same batch, which had grown in semi-controlled conditions i.e., constant organic fertilizer every 2 months and controlled drip irrigation every third day.

3.2 | Extracting the Aloe vera mucilage

After harvesting and cutting the Aloe vera plant leaves, they were washed with water to remove dirt and stored at -4°C to prevent degradation and facilitate later removal of mucilage. The removal was done using a commercial extractor (Hamilton Beach® Health-Smart, 350 w of power and two speeds, Ciudad, México) and then the pulp was centrifuged at 10000 rpm into a tabletop centrifuge (Heraeus Labofuge, model 400/400 R, USA), and later the mucilage was collected. Final pH (AOAC Technical 32,010-1984) (AOAC, *Official Methods of Analysis*, 1990), Brix degrees (Refractometer, model RF-10 with CAT, USA) and humidity (OHAUS Thermobalance MB2000, USA) measurements were 4.8%, 1.2%, and 89%, respectively. The mucilage samples contained 99.6% undiluted mucilage. Sodium benzoate and citric acid at 0.05% (w/v) were added as preservation agents.

3.3 | Ultrafiltration experiments

Figure 1 is an outline of the ultrafiltration unit used in this study.

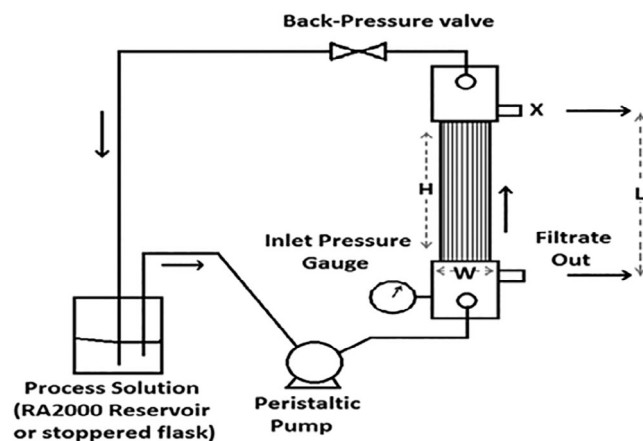


FIGURE 1 Ultrafiltration unit scheme used to concentrate the mucilage solution.

Variables considered for the UF process were: temperature (T), inlet feed rate (V), and transmembrane pressure (ΔPTM). Temperature was maintained at 25°C . Feeding rate was controlled with a peristaltic pump and input-output pressures were controlled through specific valves. Filters employed included polysulfone hollow fibers (model HIP30-43 DR4259-6 \times 3 Millipore). The UF unit dimensions have 25.4 cm width, 31.7 cm length, 26.6 cm height and 6.63 Kg weight. Peristaltic pump with variable speed, reversible of 6–600 RPM, area of 0.03 m^2 , filter length, 20.2 cm, water permeation rate (WPR), 0.07–0.15 L/min, flow rate of 22–2000 mL/min. Controls on/off switch, pump speed dial, pressure gage ranging 0–30 psi and pressure valve outlet.

3.4 | Permeate flux preparation

The permeate flux was prepared with distilled water. The first step considered a clean membrane to ensure the minimum flux resistance. The second phase consisted of passing the Aloe vera fluid through the UF unit to initiate the ultrafiltration process. After processing several mucilage concentrations, the °Brix density and rheological behavior were determined. Data collected allowed determining the flux through the membrane in the ultrafiltration process via the mathematical models.

3.5 | Rheological characterization and modeling of Aloe vera mucilage

Rheological tests were performed in a controlled stress rheometer (AR-G2, TA® Instruments of the New Castle, DE) equipped with the plate and cone geometry. Simple shear tests were performed from $\dot{\gamma} = 1\text{ s}^{-1}$ to $\dot{\gamma} = 300\text{ s}^{-1}$, flow curves were generated by plotting the apparent viscosity $\eta(\dot{\gamma})$ as a function of the shear rate $\dot{\gamma}$. Data were described using the power law and BMP models (Cervantes et al., 2014; Medina-Torres et al., 2016).

4 | RESULTS AND DISCUSSION

4.1 | Rheological properties

The viscosity curves of fresh mucilage as a function of shear rate under UF processing conditions ($T = 25^\circ\text{C}$; $\Delta P = 137.9\text{ kPa}$, $N = 160\text{ rpm}$) for the dilute and concentrated regimes (20% and 60%, respectively) are summarized in Figure 2, curves for samples at higher (60%) and lower (20%) concentration are shown. The slope of the curves does not change with the concentration, in fact, concentrated and diluted mucilage exhibit a same shear thinning behavior. Due to water removal, viscosity of concentrated mucilage is higher than diluted mucilage; however, the shear thinning behavior is not modified by the UF processes (Table 1). In Figure 2, the continuous lines represent power law predictions and dotted lines follow BMP predictions. The Power Law predictions do not able represent the behavior at high shear rates, but the BMP model follows experimental data in a more accurate way.

The power law model equation is (Medina-Torres et al., 2000; Macosko, 1994; Bautista et al., 1999):

$$\eta = k \dot{\gamma}^{(n-1)}, \quad (10)$$

where m is the consistency index (Pa s^n) and n is the shear-thinning index. Similarly, under steady state, the BMP expression has the following form:

$$\eta_{SS} = \frac{\beta \dot{\gamma}^2 \eta_0 - 1 + \sqrt{(-\beta \dot{\gamma}^2 \eta_0 + 1)^2 + 4\beta \dot{\gamma}^2 \frac{\eta_0^2}{\eta_\infty}}}{2\beta \dot{\gamma}^2 \frac{\eta_0}{\eta_\infty}}, \quad (11)$$

where β (Pa^{-1}s) or $\beta = \lambda k$ is a kinetic-structural parameter, i.e., the product of the structural relaxation time (λ) and the kinetic constant for rebuilding (k); η_0 and η_∞ are the viscosity at zero and high shear rates, respectively.

The BMP model describes satisfactorily the experimental data better than the power law predictions at high shear rates. According

to the results, the mucilage is a highly pseudoplastic fluid ($n < 1$) since its viscosity changes rapidly with shear. Moreover, the consistency indices are functions of concentration in the UF process. Data suggests that UF does not modify the pseudoplastic character of the mucilage, since the shear thinning index remains constant. The UF process increases the consistency index of the mucilage in approximately 1000%. In general, the rheological behavior of the mucilage of Aloe vera is similar to other food fluids, fruits, and nopal mucilage (*Opuntia ficus-indica*), which are also pseudoplastic (Medina-Torres et al., 2000). For example, nopal mucilage (*Opuntia ficus-indica*) has values of $n = 0.56$ and $m = 0.15\text{ Pa s}^n$ at 3% (w/v), concentrated tomato obtained by filtration has values of $n = 0.59$ and $m = 0.22\text{ Pa s}^n$ and banana concentrate has values of $n = 0.458$ and $m = 6.51\text{ Pa s}^n$ (Medina-Torres et al., 2000; Aymar, 1987; Pritchard, 1990). The high pseudoplasticity level found in the mucilage influences strongly the UF process. The modeling of the ultrafiltration process with the BMP equations has not been previously reported.

4.2 | Water permeation (AOAC)

Characterization of the membrane included permeate flux measurements with distilled water, prior to the mucilage concentrate experiments. Experimental data for the permeate flux with water were taken at steady state. UF operating conditions are presented in Figure 3. Data suggest that steady state is reached past the first 5 min of the process initiation. The water permeate flux under steady state is 144 L/h m^2 , which lies within the range given by the manufacturer of $130\text{--}180\text{ L/h m}^2$.

4.3 | Aloe vera mucilage permeate

Experimental data under steady state of fresh mucilage under operation conditions such as those employed with pure water are shown in

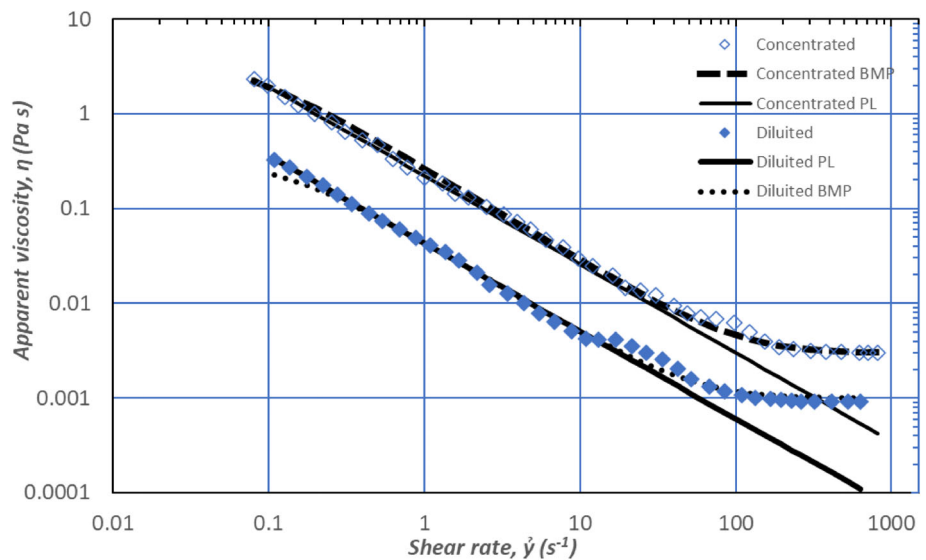


FIGURE 2 Rheological parameters of power law and BMP models of fresh mucilage under UF processing conditions (i.e., $T = 25^\circ\text{C}$; $\Delta P = 137.9\text{ kPa}$, $N = 160\text{ rpm}$) at two concentrations: concentrated (filled rectangles) and diluted (hollow rectangles) mucilage regimes.

TABLE 1 Rheological parameters for different rheological models of Aloe vera solutions.

Rheological model	BMP				PL		
	η_0 (Pa s)	η_∞ (Pa s)	β (Pa ⁻¹ s)	Standard deviation σ	k (Pa s ⁿ)	n	Standard deviation σ
Diluted Mucilage	0.32	0.001	0.047	0.02138	0.0429	0.07	0.0061
Concentrated Mucilage	3.7	0.003	0.040	0.05570	0.2225	0.07	0.3039
R^2	Diluted mucilage		Concentrated mucilage		Diluted mucilage	Concentrated mucilage	
	0.94216		0.9919		0.9671	0.9802	

Adjusted R^2 and the standard deviation of goodness-of-fit.

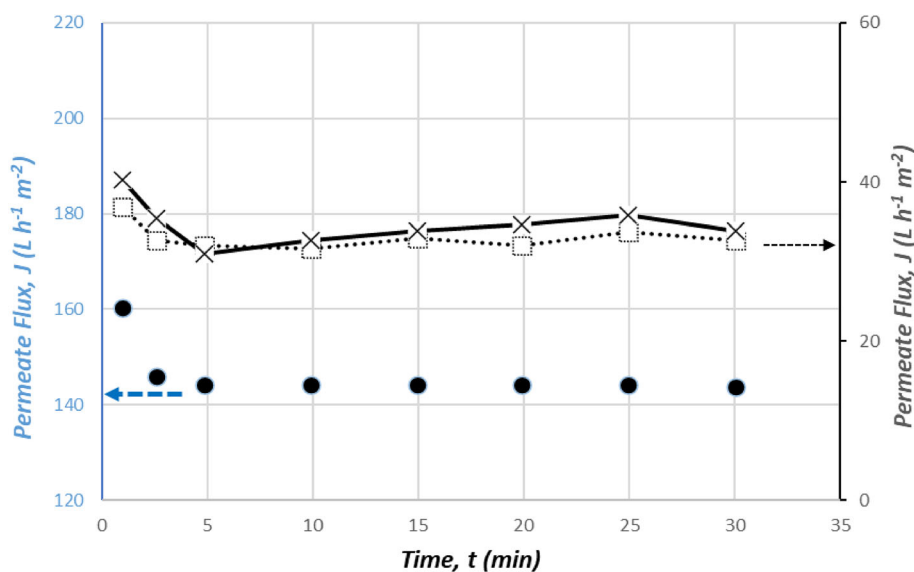
**FIGURE 3** Permeate flux measurements J (L/m² h) with distilled water (filled circles), and concentrated (crosses and solid line) and non-concentrated (hollow rectangles and dotted line) of Aloe vera mucilage at steady state as a function of operating time (min) of UF processes.

Figure 3, where concentrated (crosses and solid line) and non-concentrated (hollow rectangles and dotted line) solutions, respectively. Data suggest that steady-state was reached past the first 5 min of process initiation. Although the value of the permeate flux (34.2 L/h m²) greatly differs from that of water (144 L/h m²), this permeate flux is still below the nominal value given by the manufacturer but suitable for the UF process. The permeate flux as a function of the mucilage concentration is presented in Figure 4, where an indirect relation is found, that is, as the concentration increases, the permeate flux decreases.

4.4 | Rheological modeling of UF process

Rheological modeling of UF process of non-Newtonian fluids through membranes is still incipient. Insight work is required to predict the performance of a given membrane and fluids in terms of flux and influencing variables (i.e., mass transfer coefficient, k ; pressure drop, ΔP ; viscosity of filtrate, η ; and membrane area, A). In particular, reports in the literature have been devoted to the prediction of the convective mass transfer coefficient, k . Many correlations have been developed for heat transfer in non-Newtonian fluids (e.g., Equation 9a) usually for conditions where $K_w < K_b$. Membrane

conditions involve the cases where $K_w > K_b$. Moreover, pseudoplastic properties of a fluid may be independent of temperature and these correlations only consider the case of the boundary layer having the same degree of pseudoplasticity as the bulk fluid (Mondal et al., 2016).

The model proposed by Charcosset and Choplin (1996) is based on heat transfer analogies in pseudoplastic fluids, where viscosity remains high in the pipe center and decreases toward the wall. The flow of a pseudoplastic fluid in a tube is then characterized by an almost plug flow in the central region surrounded by a low viscosity fluid. Combining the Newtonian equivalent viscosity in the bulk and the apparent wall viscosity at the membrane surface, the following mass transfer coefficient expression is obtained:

$$k = \left(\frac{3D^2}{4L} \right)^{1/3} \left(\frac{3n_b + 18u}{4n_b} \right)^B \left(\frac{3n_w + 1}{4n_w} \right)^{0.27(1-n_w)} \left(\frac{3n_b + 1}{4n_b} \right)^{0.27n_w} \left(\frac{m_b}{m_w} \right)^{0.27}, \quad (12)$$

where n_b , n_w , m_b , and m_w represent the flow index (n) and consistency (m) at the center (b) and walls (w) of the pipe; D is the diffusion coefficient of the solute, u , L , and d , are ascribed to velocity, membrane length, and the diameter of the tubular membrane, respectively. B is the coefficient of the axial speed, given by:

FIGURE 4 Permeate flux as a function of the mucilage concentration (%).

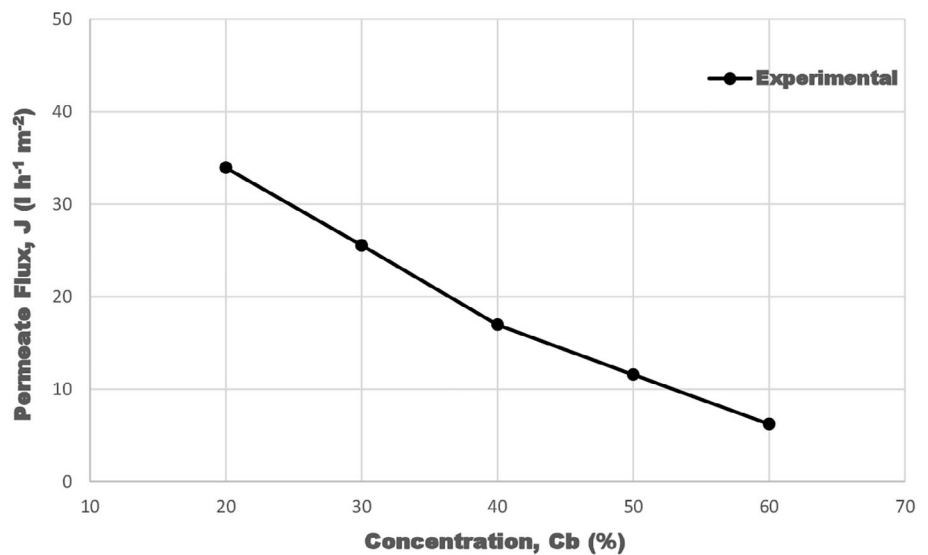


TABLE 2 Results of permeate flux prediction employing the rheological parameters.

Concentration C_b (%)	Exp. data, J ($l\ h^{-1}\ m^{-2}$)	Power law model, J ($l\ h^{-1}\ m^{-2}$)	Absolute average error (%)	Standard deviation σ	BMP model, J ($l\ h^{-1}\ m^{-2}$)	Absolute average error (%)	Standard deviation σ
20	33.94	34.14	26.41	11.79	38.30	15.98	15.14
40	16.97	20.21			18.09		
60	6.23	9.93			7.25		

Absolute average error of model prediction and the standard deviation of goodness-of-fit.

$$B = \frac{1}{3} + 0.27(n_b - n_w). \quad (13)$$

Exponent B varies from 0.6 in the Newtonian case to 0.33 in the highly pseudoplastic case (i.e., when the flow index is small). Notice that coefficient B decreases as the degree of pseudoplasticity increases or the mucilage concentration increases. The convective mass transfer coefficients were estimated using an appropriate algorithm employing the different rheological models. The results of flux prediction for power law and BMP models are shown in Table 2. The absolute average error is reported for comparison between the power law and BMP models. The BMP model shows a lower error in predicting the permeate flux predictions at all mucilage concentrations.

Figure 5a,b depicts the axial speed exponent “ B ” and flow index “ n ” as functions of mucilage concentration “ C_b ”. In general, both parameters decrease as the mucilage concentration increases, indicating that the fluid becomes more pseudoplastic ($n < 1$) and thus with lower coefficient of the axial speed “ B ”, reaching a limiting value of 0.33 in the case of highly concentrated mucilage. There is a notable change in slope in Figure 5a,b at 40%, observed at a critical mucilage concentration (i.e., semi-dilute to concentrated regime transition) where particles in the solution interact with each other strongly and thus the pseudoplasticity of the fluid does not decrease fast enough as in the concentrated regime.

This study is based on a more consistent description of the complex rheology with respect to that predicted by the power law

description of Charcosset and Choplin (1996). Using the BMP model, the following expression for k_c is obtained (see Appendix S1):

$$k_c = \left(\frac{3D^2}{4L} \right)^{\frac{1}{3}} \left(\frac{8u}{d} \right)^{\frac{1}{3}} \left(\frac{\eta_{PN}(C_b)}{\eta_{ab}(C_w)} \right)^{0.27}, \quad (14)$$

where $\eta_{PN}(C_b)$ and $\eta_{ab}(C_w)$ are the Newtonian viscosity in the bulk and the apparent wall viscosity at the membrane surface, respectively (see Equation A).

UF process predictions of the two models are shown in Figure 6 (Permeate flux) and Figure 7 (mass transfer coefficient) as a function of the mucilage concentration (%). The continuous line follows the experimental points; the dashed line depicts power-law predictions, and the dotted line follows predictions of the BMP model. Figure 6 shows that the BMP model represents the Permeate flux better than the power law model specially at high mucilage concentration.

Finally, Figure 7 reports the prediction of the mass transfer coefficient as a function of mucilage concentration. Here, the need of more complex rheological models is clear since the power law predicts an increase in the mass transfer coefficient as concentration increases which is clearly not the case. BMP model represents better the behavior of the mass transfer coefficient that is independent of the mucilage concentration. Table 3 shows the comparison of both models regarding the mass transfer coefficient prediction. The BMP model describes better the experiments of permeate flux of the mucilage with lower absolute error than those using power law (see Tables 2 and 3).

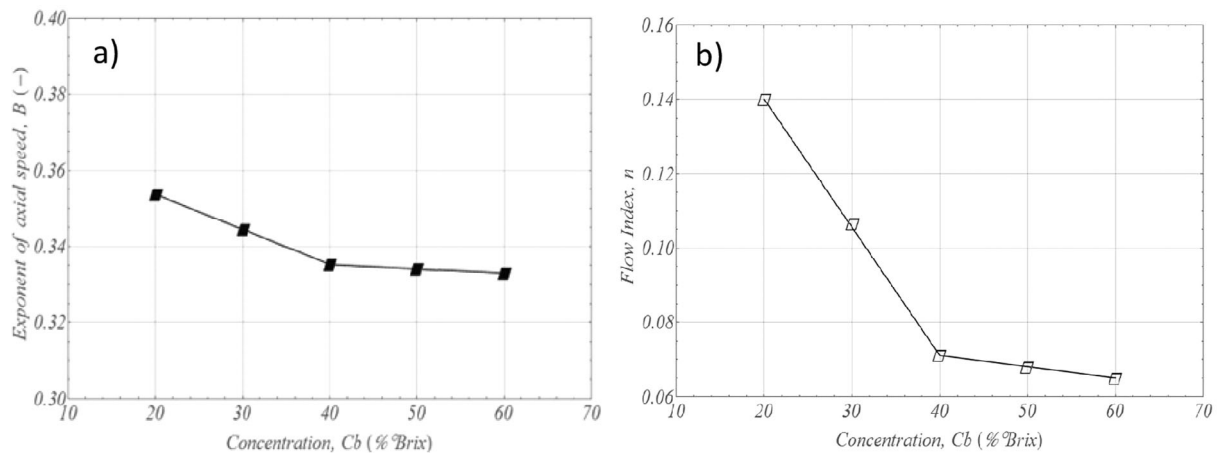


FIGURE 5 (a) Prediction of the exponent B of the axial velocity term as a function of the mucilage concentration ($^{\circ}$ Brix). (b) Flow index (n) of the power law model as functions of mucilage concentration " C_b " using the model of Charcosset and Choplin (1996).

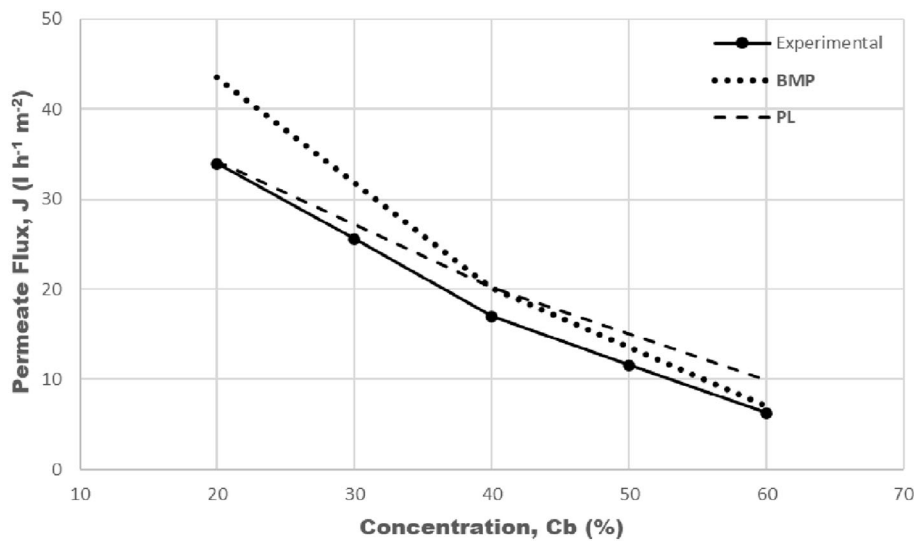


FIGURE 6 Permeate flux prediction for UF of Aloe vera mucilage (continuous line follows the experimental points; the dashed line depicts power law predictions, and the dotted line follows predictions of the BMP model).

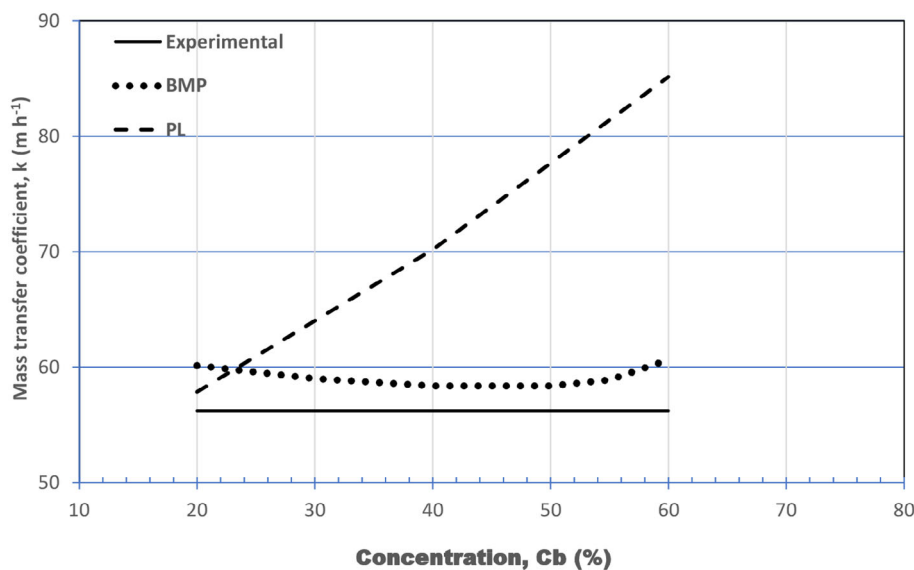


FIGURE 7 Mass transfer coefficient prediction for Aloe vera mucilage in the UF process (Continuous line follows the experimental points; the dashed line depicts power law predictions, and the dotted line follows predictions of the BMP model).

TABLE 3 Mass transfer coefficient prediction for Aloe vera mucilage and UF concentrate employing rheological models (power law and BMP predictions).

Concentration C_b (%)	Exp. data, k ($m\ h^{-1}$)	Power law model, k ($m\ h^{-1}$)	Absolute average error (%)	Standard deviation, σ	BMP model ($m\ h^{-1}$)	Absolute average error (%)	Standard deviation, σ
20	56.2	57.84	26.42	22.74	60.13	8.70	4.62
40	56.2	70.17			58.99		
60	56.2	85.13			60.62		

Absolute average error of model prediction and the standard deviation of goodness-of-fit.

5 | CONCLUSIONS

Ultrafiltration processes in Aloe vera mucilage solutions produce a change in the consistency index “ β ” by approximately 1000% upon increasing concentration, preserving the shear thinning behavior. This is an indication of small structural changes with moderate damage of polysaccharides. Since high molecular weight compounds are highly sensitive to shear and temperature, the UF process represents an advantage in comparison to traditional concentration methods, producing a higher quality mucilage.

Power law predictions of the permeate flux are good at low concentrations and those of the proposed model (BMP) are better along the medium-high concentration range, where the rheological behavior is more complex.

Experimental data for the ultrafiltration process are described efficiently by the polarization model. Predictions of permeate flux in complex fluids, namely, pseudoplastic fluids, are crucial to optimize and better design of UF processes as alternatives to well-established concentration methods (e.g., traditional filtration). In this context, predictions of the BMP model are highly suitable in the description of real systems as the concentration of the mucilage increases, compared with those of the traditional power law model.

This study represents an interesting and promising alternative to estimate the permeate flow as a function of the concentration of Aloe vera mucilage by using more realistic rheological models with promising applications in the food industry.

CONFLICT OF INTEREST STATEMENT

The authors would like to state that there is no conflict of interest of any kind, and ethics approval was not required for this research. All the authors listed made substantial contributions to the manuscript and qualify for authorship, and no authors have been omitted. We warrant that all the authors have agreed to this submission.

DATA AVAILABILITY STATEMENT

The data that support the findings of this study are available from the corresponding author upon reasonable request.

ORCID

L. Medina-Torres  <https://orcid.org/0000-0002-9963-821X>

F. Calderas  <https://orcid.org/0000-0002-3652-4223>

REFERENCES

- Aimar, P. (1987). Ultrafiltration of pseudoplastic fluids. In M. S. Verall & M. J. Hudson (Eds.), *Separations for biotechnology* (pp. 360–372). Ellis Horwood.
- AOAC. (1990). *Official methods of analysis*. Association of Official Analytical Chemists Printed in the N.Y. of United States of America. ISBN: 0-935584-42-0.
- Bautista, F., de Santos, J. M., Puig, J. E., & Manero, O. (1999). Understanding thixotropic and antithixotropic behavior of viscoelastic micellar solutions and liquid crystalline dispersions. I. The model. *Journal of Non-Newtonian Fluid Mechanics*, 80(2-3), 93–113.
- Cervantes, C. V., Medina-Torres, L., González-Laredo, R. F., Calderas, F., Sánchez-Olivares, G., Herrera-Valencia, E. E., Gallegos Infante, J. A., Rocha-Guzmán, N. E., & Rodríguez-Ramírez, J. (2014). Study of spray drying of the Aloe vera mucilage (*Aloe vera barbadensis miller*) as a function of its rheological properties. (LWT). *Food Science and Technology*, 55(2), 426–435. <https://doi.org/10.1016/j.lwt.2013.09.026>
- Charcosset, C., & Choplin, L. (1996). Ultrafiltration of non-Newtonian fluids. *Journal of Membrane Science*, 115(2), 147–160.
- Cheryan, M. (1986). *Ultrafiltration handbook*. Technomic Publishing Co. Inc ISBN: 87762-456-9.
- Chou, F., Wiley, R. C., & Schlimme, D. V. (1991). Reverse osmosis and flavor retention in apple juice concentration. *Journal of Food Science*, 56(2), 484–487.
- Cui, Z. F., Jiang Y., & Field R. W. (2010). *A practical guide to membrane technology and applications in food and bioprocessing*. In Z. F. Cui & H. S. Muralidhara (Eds.), (1st ed., ISBN: 9780080951348, p. 12). Membrane Technology.
- Femenia, A., García-Pascual, P., Simal, S., & Rosselló, C. (2003). Effects of heat treatment and dehydration on bioactive polysaccharide acemannan and cell wall polymers from *Aloe barbadensis* Miller. *Carbohydrate Polymers*, 51(4), 397–405.
- Femenia, A., Sánchez, E. S., Simal, S., & Rosselló, C. (1999). Compositional features of polysaccharides from Aloe vera (*Aloe barbadensis* Miller) plant tissues. *Carbohydrate Polymers*, 39(2), 109–117.
- Lim, Y. P., & Mohammad, A. W. (2012). Influence of pH and ionic strength during food protein ultrafiltration: Elucidation of permeate flux behavior, fouling resistance, and mechanism. *Separation Science and Technology*, 47(3), 446–454.
- Macosko, C. W. (1994). *Rheology: Principles, measurements and applications*. VCH ISBN: 978-0-471-18575-8.
- Mears, P. (1976). *Membrane separation processes*. Elsevier Scientific Publishing, N.Y. ISBN: 9780444816337.
- Medina-Torres, L., Brito-De La Fuente, E., Torrestiana Sánchez, B., & Katthain, R. (2000). Rheological properties of the mucilage gum (*Opuntia ficus indica*). *Chemistry Hydrocolloids*, 14, 417–424.
- Medina-Torres, L., Calderas, F., Minjares, R., Femenia, A., Sánchez-Olivares, G., González-Laredo, F. R., Santiago-Adame, R., Ramírez-Núñez, M., Rodríguez-Ramírez, J., & Manero, O. (2016). Structure preservation of Aloe vera (*barbadensis* Miller) mucilage in a spray drying process. *LWT-Food Science and Technology*, 66, 93–100.

- Mondal, S., Cassano, A., Conidi, C., & De, S. (2016). Modeling of gel layer transport during ultrafiltration of fruit juice with non-Newtonian fluid rheology. *Food and Bioproducts Processing*, 100(2016), 72–84.
- Muller, H. (1982). *Introducción a la Reología de los Alimentos*. Acribia.
- Nakao, S. I., Nomura, T., & Kimura, S. (1979). Characteristics of macromolecular gel layer formed on ultrafiltration tubular membrane. *American Institute of Chemical Engineers*, 25(4), 615–622.
- Pizzichini, M. (1995). Membrane application in food industry. In *Membrane technology: Applications to industrial* (pp. 151–174). Wastewater Treatment Springer.
- Pritchard, M. (1990). The influence of rheology upon mass transfer in cross-flow membrane filtration (Doctoral Dissertation, University of Bath).
- Rodríguez-Rodríguez, E., Darias Martin, J., & Díaz Romero, C. (2010). Aloe vera as a functional ingredient in foods. *Critical Reviews in Foods Science and Nutrition*, 50, 305–326.
- Vega, G. A., Ampuero, C. N., Díaz, N. L., & Lemus, R. M. (2005). El Aloe Vera (*Aloe Barbadensis* Miller) como Componente de Alimentos Funcionales. *Revista Chilena de Nutrición*, 32, 27–33.

SUPPORTING INFORMATION

Additional supporting information can be found online in the Supporting Information section at the end of this article.

How to cite this article: Medina-Torres, L., Guillen, I. H. G., Núñez-Ramírez, D. M., García-Guzmán, P., Calderas, F., González Laredo, R. F., Gonzalez Lozano, M. A., Ramirez Torres, L. A., & Manero, O. (2023). Rheological behavior and modeling of an ultrafiltration process for Aloe vera. *Journal of Food Process Engineering*, e14416. <https://doi.org/10.1111/jfpe.14416>